Acta Polytechnica CTU Proceedings **38**:247–254, 2022
https://doi.org/10.14311/APP.2022.38.0247
© 2022 The Author(s). Licensed under a CC-BY 4.0 licence
Published by the Czech Technical University in Prague

PRVOK – ISSUE ON 3D PRINTING CONCRETE BUILDING

Kateřina Nováková[a,*], Jiří Vele[a], Jiří Litoš[b], Vladimír Šána[b]

[a] *Czech Technical University in Prague, Faculty of Architecture, Thákurova 9, 166 34 Prague 6, Czech republic*
[b] *Czech Technical University in Prague, Faculty of Civil Engineering, Thákurova 7, 166 34 Prague 6, Czech republic*
[*] corresponding author: katerina.novakova@fa.cvut.cz

Abstract. Prvok is the first 3D printed concrete floating house in the Czech republic. Additive manufacturing – 3D printing became a synonym of sustainable building of the 21st century. Its experimental manner and lack of world's standardisation ISO approvals hold the 3D printing concrete method on the edge of usability and applicability and stop a broader spread of application in practice. Furthermore, the used material was newly developed cement composite prefabricated mixture mady by Master Builder Solutions with polypropylene plastic micro-fibres, which was not previously tested in large structures. What we achieved, was a practical realisation of a 3D printed fully equipped and functioning concrete house as a habitable statue for a public event. In order to fulfil the request on insulation and avoiding heat bridges together with investing least material possible, we parametrically designed and implemented a wall system of construction. In order to be able to open the structure to the public, we tested it on the universal loading machines at the Faculty of civil engineering CTU Prague in scale 1:1. Testing fragments of the walls were also part of the research goals, which led us to the final design. In this paper, we present the results of the experiment together with the experimentally obtained data.

Keywords: 3D printing, concrete, prefabricated cement composite, parametrically designed self load-bearing structure, static loading tests.

1. Introduction

We can follow the evolution of 3D printing concrete structures since 2014 [1], when the Centennial Challenge [2] for 3D-Printed Habitat was announced by the NASA in the USA. This competition started a race for technological principles and optimal material mixtures for the use in additive manufacturing method of constructing a habitat. The winners of various stages of different phases of the challenge including Pennsylvania State University team [3], Foster and Partners [4] and Al space Factory [5] published the results throughout 5 years long lasting challenge. We could see that these structures had had initially a circular geometry with the thickness of 6 layers generating at least 30 cm thick walls. It took two years till first inhabitable commercially 3D printed structure called "Office of the future" made by WinSun – Yingchuang Suzhou factory appeared in Dubai [6]. Still, combination of robotic and manual work is inevitable [7] together with experiments on the site during the building process. The inner structure consisting of two walls being laterally supported by inner zigzag was adopted by further realisations. Although structural tests proved its stability, this system still had the problem of heat bridges. In 2017 an article about a first 3D printed house made by American company ApisCor was published [8]. While previous examples were mounted from prefabricated panels, the construction system introduced by Nikita Cheniuntai was focused on printing on the site. This minimised required construction space and transportation demands. A different attitude was shown in Yhnova House in 2017 [9], where the structure of foam insulation was 3D printed, filled with concrete and reinforced with classical steel caging column structure. Although after 2018 many realisations appeared, this did not lead to ASTM standardisation of mixtures, structures, thicknesses or reinforcement of the walls. Mechanical properties of 3D printed concrete specimen were tested and compared with monolithic specimen [10]. Anyway, these samples were cut into small standard cubes. Furthermore, the 3D printed samples could be negatively influenced by the process of cutting.

Firstly, this article is investigating the problem of difference between virtual model (digital twin) and robotically manufactured prototype. Next, his paper is describing the structure and testing of the load bearing wall, which has different geometry than above mentioned walls known so far. Finally, the article mentions possible wall stabilisation method during the printing process.

2. Differences between 3D printed object and its digital twin

We noticed discrepancies between printed object – Prvok (Figure 1) and its digital twin. Here we understand the digital twin as a real-time digital counterpart of a physical object. Our hypothesis expected the real object to be almost precise copy of its virtual model.

Figure 1. Prvok 1:1 3D printed structure.

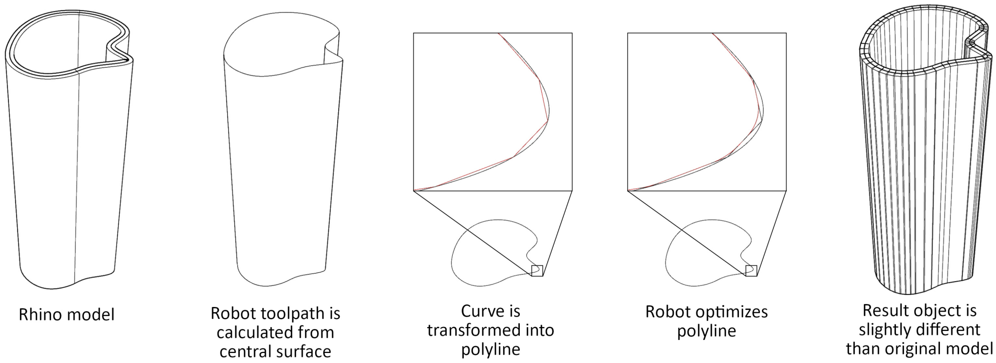

Figure 2. Robot optimization of the path.

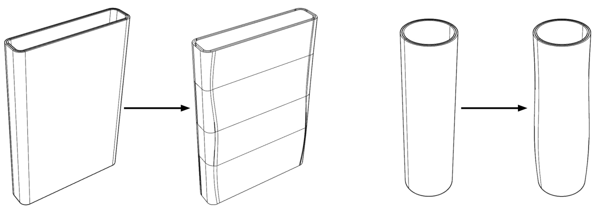

Figure 3. The principle of buckling.

Figure 4. Buckling of the 3 meter high wall.

2.1. Buckling

It is well known [10] there are certain threats of buckling, which is understood as deformation of a structural component of 3D printed objects (Figure 3). In our case, on a 3 m tall wall buckling caused 3 cm difference from 3D model (Figure 4). Interior of Prvok was designed as very curvy space and it required e.g. special shaped kitchen surface, shelves, bed, etc. In order to save construction time, curves of this equipment were exported from Rhino model and its parts were cut in advance on the CNC machine. But finally the 3D printed walls had different curvature than CNC-cut wood. So the 3D printed walls had to be scanned and new wooden parts were cut. It slowed down the manufacturing process and disapproved the advantages of automated construction, which made us investigate the problem.

2.2. Digital model versus manufacturing process

Changes happened in data preparation. We used Grasshopper for converting Rhino model to Robots Move L instructions. Grasshopper derived a curve from Rhino model. This curve performed as robot toolpath, but robots instructions were linear movements, so curve was transformed into poly-line of multiple straight segments. If two segments of poly-line had sharp angle, robot readjusted its movement to keep continuous speed and did not follow the exact path of the poly-line. Instead, the robot went through the

Figure 5. Optimal consistent material (left) and inconsistent material (right).

Figure 6. Printed segment of the PRVOK.

zone around desired point. The zone is a circular area around all points on the poly-line. In our case, the zone diameter was 15 mm.

Average width of each layer is 4.5–5 cm, but if a printing mixture is inconsistent due to fluctuating liquidity, width may differ from 4 to 6 cm. The more liquid mixture is the easier the pumping is and more material is being extruded, which is resulting in layer width around 6 cm. More liquid layers have longer setting time and collapse may happen. Less liquid mixture is difficult to pump, so less material is extruded, resulting in layer widths around 4 cm. Dry layers crack during the printing and they are not properly bonded with other layers. These are weak spots of structure and if cracks appear, they usually follow these weak layers (Figure 5).

Plus there are other problems with manufacturing process, which cause the different geometry of the prototype (Figure 2). For example, the 3D printing mixture Master Flow 100 is very sensitive to temperature and humidity changes. If uncontrolled temperatures happen to be below 15 °C, the accelerant does not work and it takes too long time for concrete to get solid. Thus, under 15 °C any object collapses during the printing.

Furthermore, freshly printed structures sometimes deform under its self-weight. The scale of deformation is affected by the shape of printed object and by printing speed, ideally higher that 60 s. The longer it takes to print one layer, the more time is given to the fresh concrete to bond the layers in order to gain strength. Generally, the conclusion is that objects with small layout have to be printed slowly (60 s speed +), or in segments. Complexity of geometry also plays significant role. Our observation claims, that straight walls or walls with big radius in plane view tend to deform. This is the reason why external walls of Prvok are double curved (Figure 6) and interior ones are straight, but supported by small circular shapes (Figure 7). We printed hidden column each 500 mm of the path in order to stabilize the wall during the printing process. After the construction dried, steel

Figure 7. Construction of the wall during the printing.

Figure 8. Load distribution system.

rebars with liquid concrete mixture were installed into these spaces in order to reinforce the walls against deformation.

3. Geometry of the walls and compressive tests of the prototype

Part of the whole building made of cement composite was printed at the Experimental Centre of the CTU in Prague, Faculty of Civil Engineering. Static loading test of compressive load capacity and a stability test of the structure were performed.

The subject of the static loading test was a 3D printed part of the building (Figures 7 and 9). It was 3D printed using a robotic arm. A specially developed cementitious composite material Master Flow 100 was used as the printing medium. The wall of the structure was divided into two types of walls. Firstly, an external self-supporting part, which gave the building characteristic wavy illusion. Secondly, an internal load-bearing part reinforced with ribs (Figure 7), on which the roof trusses were placed. The subject of the static load test was the internal load-bearing part of the wall. The height of the printed structure was 2.8 m and its enclosed area was 10 m^2. The thickness of the printed shell ranged from 50 to 60 mm and the thickness of the whole wall ranged from approximately 350 to 450 mm.

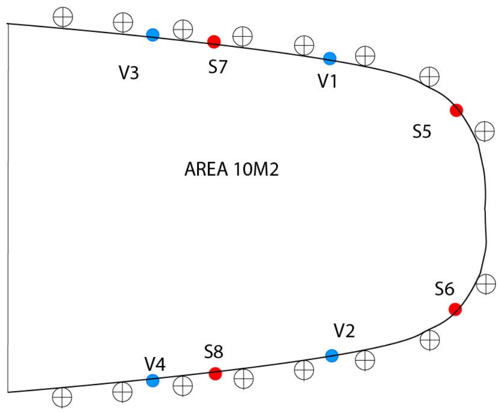

Figure 9. Measuring points of vertical and horizontal deformations.

Using a system of spreader arms, the load from one load hydraulic cylinder was distributed to 16 locations on the structure (see Figure 8), with each of these locations being loaded with the same amount of force. The load locations were the positions of the future roof trusses.

During the static loading test, vertical and horizontal deformations of the structure were measured. Furthermore, the load force and the path of the load cylinder, was monitored. Vertical deformations (compression along the height of the structure) were recorded

Load steps	Load description	Load force – spreading elements and hydraulic system [kN]	Surface load [kN/m^2]
0	Spreading elements	12	1,2
1	Roof sheathing	21	2,1
2	Increase by snow load – (hidden ref.) area	29	2,9
3	Increase by accidental load	41	4,1
4	Roof sheathing	21	2,1
5	Increase max value by 10 kN	52	5,2
6	+10 kN	62	6,2
7	+10 kN	72	7,2
50	Limit of the spreading elements	500	50

Table 1. The load stages.

at four locations labelled from S5 to S8. The horizontal deformations were measured at points located at the mid-height of the structure labeled from V1 to V4 (see Figure 9).

Verification of the load capacity of the printed structure was carried out successively in three loading steps. The loading of the structure was controlled by gradually increasing the loading force at a rate of 5 kN/min. The first step represented the dead load of the roof structure (21 kN). In the second loading step, the force was increased by the load of snow for the central Czech area (+8 kN) and the last step increased the loading force by the value of the accidental load (+12 kN). Subsequently, the structure was unloaded to the first step load value. At each loading step, the load was maintained for two minutes to allow the measured values to settle. After this part of the load test, the structure was progressively loaded up to 500 kN in 10 kN increments and held at each load for one minute. After this maximum value was reached, the structure was fully unloaded. The load on the hydraulic load cylinder had to be increased by the load from all the spreading elements, which was 12 kN. The individual load stages are summarised in the Table 1 and Figure 10. The table shows the values of the hydraulic load cylinder and also the values converted to the surface load of the structure, where the area of the printed part was 10 m^2.

The results of the static loading test can be seen in the graphs (Figure 10 and 11). Graph on Figure 11 shows the vertical deformations during loading of the structure. Graph on Figure 12 then shows the horizontal wall deflections. The deformations are then shown in Table 2. The values marked from V1 to V4 are the horizontal wall deflections, where a positive sign of the value indicates buckling of the structure towards the living space. The values marked from S1 to S4 indicate compression of the load-bearing part of the structure. Almost no vertical or horizontal deformations were measured during the static load test that was intended to verify the load-bearing capacity of the structure (Table 2). Permanent deformations after unloading are negligible (see step 4).

The next load steps show deformation values where the structure was progressively loaded to a value exceeding ten times the required load capacity of the printed structure. In this case, the values were already measurable, but as in the previous case and due to the size of the structure, negligible. Load step 51 then indicates the permanent deformation of the structure after the load force has been fully relieved.

4. Compressive strength of specimen

In the last test session, 1×1 m specimen made of MBS material [11] were generated from the big structure. The measurement was performed on samples printed by a 3D printer and cut from a 1:1 scaled model after static loading test. At first, we had measured the quantity and thickness of individual connections of printed layers on 8 samples (marked in the table with numbers from 1–8) with average dimensions 127.55×74.96 mm and a weight with an average of 0.91 kg (Figure 13). The result of measuring the thickness of the connection was used to determine the narrowest location, which we assumed to be the weakest point on each sample. Subsequently, we performed a destructive test on all samples at this point on a pressure press and calculated the individual compressive strengths (MPa) according to the appropriate well-known formula.

5. Discussion and conclusion

In Lee at al. [10] several contradictory statements from previous research are reported. For example, Wolfs et al. [12] states, that the direction of the printed layers has minimum effect on the mechanical properties of the specimen [12] but Nerella et al. [13] reports, that the effect is significant. In our experiment, we measured almost same values of compressive strength as in Lee at al. [10] 21.4 MPa versus 23.5 MPa is within standard deviation of ±5.4 MPa. Because of the nature of the experiment (top-bottom stress), only one direction of specimen-load was measured with positive result.

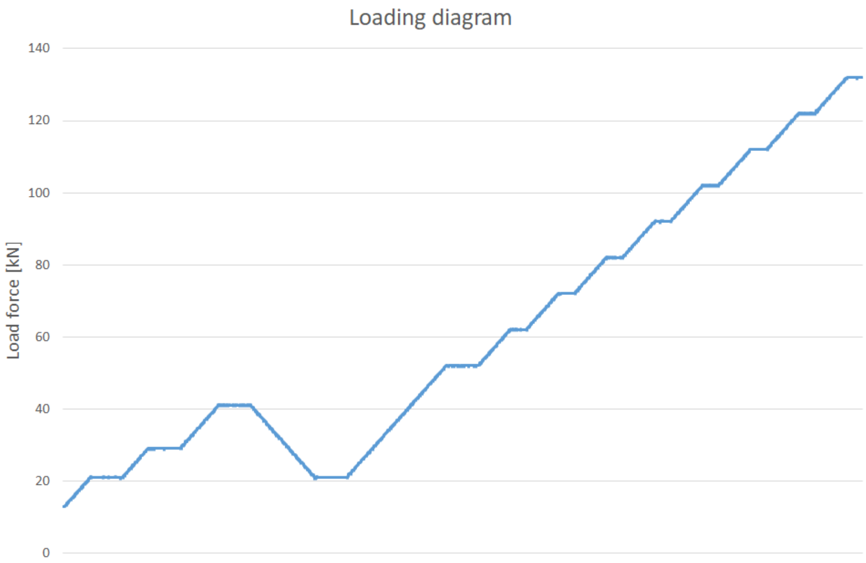

Figure 10. The loading diagram.

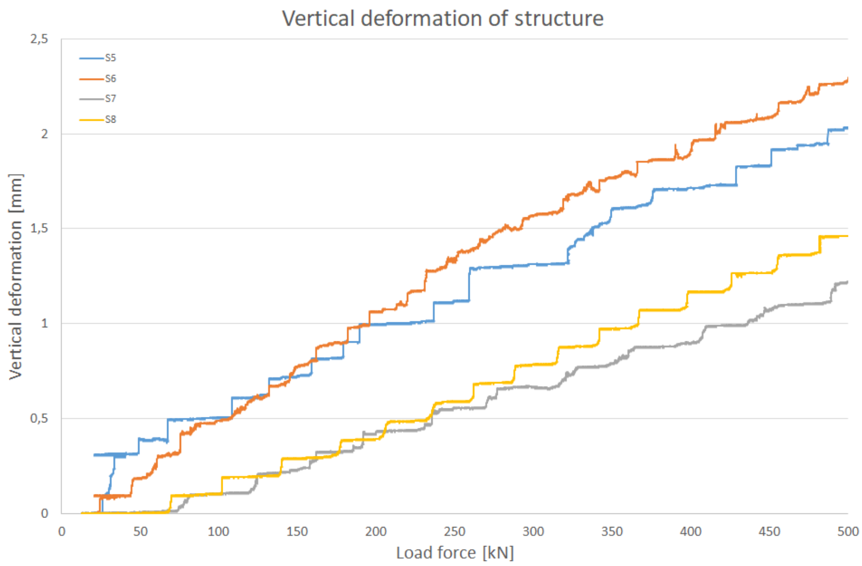

Figure 11. The vertical deformation.

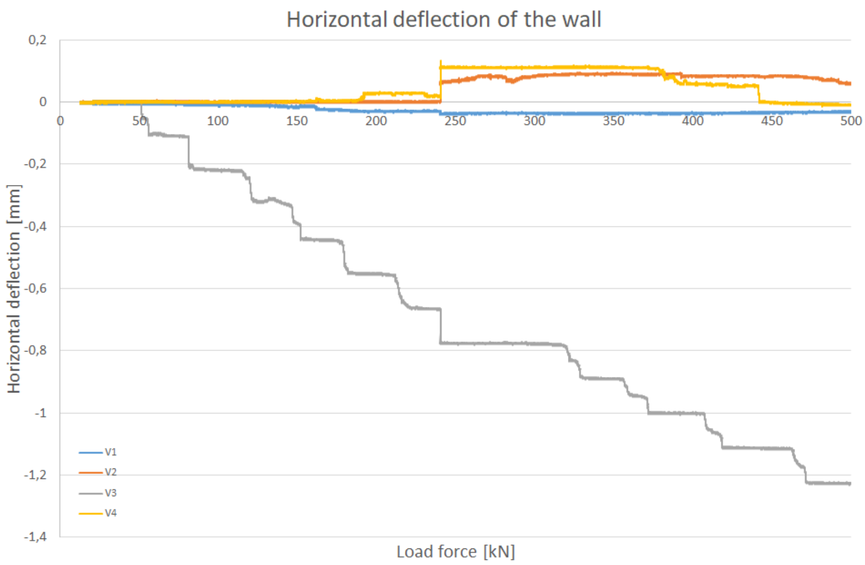

Figure 12. The load stages.

Load step	Load force [kN]	V1	V2	V3	V4	S1	S2	S3	S4
1	21	0.00	0.00	0.00	0.00	0.00	0.00	0.00	0.00
2	29	0.00	0.00	0.00	0.00	0.11	0.08	0.00	0.00
3	41	0.00	0.00	0.00	0.00	0.32	0.09	0.00	0.00
4	21	0.00	0.00	0.00	0.00	0.31	0.09	0.00	0.00
10	100	0.00	0.00	-0.22	0.00	0.61	0.54	0.11	0.19
20	200	-0.02	0.00	-0.57	0.03	1.00	1.08	0.44	0.48
30	300	-0.04	0.09	-0.78	0.11	1.32	1.58	0.66	0.79
40	400	-0.03	0.08	-1.05	0.05	1.72	1.97	0.99	1.17
50	500	-0.03	0.06	-1.29	-0.01	2.03	2.36	1.22	1.56
51	12	-0.05	0.06	-0.45	-0.01	0.52	1.12	0.1	0.19

Table 2. Measured deformations during individual load steps [mm].

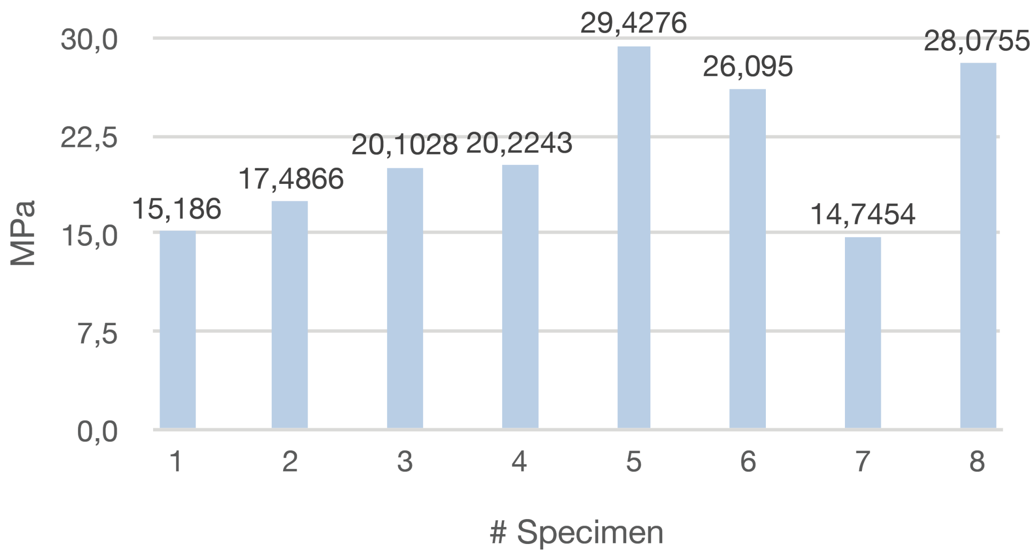

Figure 13. The compressive strength of experimentally investigated specimen.

	μ [MPa]	s [MPa]
The compressive strength	21.4	±5.4

Table 3. Summarization of evaluated compressive strength. The symbol μ denotes the mean value and s is the standard deviation.

The conclusion says, that physical result of digital fabrication process differs from the virtual model. We observed, that the digital twin has two main sources of imperfection: The logic encoded in data transfer from a model to robots' nozzle and the irregular and hardly controllable consistency and flow of the actual mixture in the process of layering. Nevertheless, we can see, that the compressive strength of our samples is comparable with the results referenced below [10]. Also the 1:1 stress test has proven satisfactory resilience for the conditions of Czech Republic. Therefore, even though the actually 3D printed structure deviates from the original digital model it is structurally very solid and exceeds many times the required limits of safe structures. This implies the conclusion, that the effect of imperfect printing and inaccurate digital twin does not influence the overall strength of the building.

Acknowledgements

This research has been supported by the CTU in Prague and by the Ministry of Education, Youth and Sport of the Czech Republic within INTER EXCELLENCE program, under project No. LTAUSA19018.

References

[1] M. Rešetár. *Architektura 3D tlače*. Batchelors work, CTU Prague, 2021.

[2] T. Prater, T. Kim, M. C. Roman, R. P. Mueller. NASA's centennial challenge for 3D-printed habitat: Phase II outcomes and phase III competition overview. In *2018 AIAA SPACE and Astronautics Forum and Exposition*. 2018. https://doi.org/10.2514/6.2018-5405

[3] N. D. Watson, N. A. Meisel, S. G. Bilén, et al. Large-scale additive manufacturing of concrete using a 6-axis robotic arm for autonomous habitat construction. In *Solid Freeform Fabrication 2019: Proceedings of the 30th Annual International Solid Freeform Fabrication Symposium – An Additive Manufacturing Conference*. 2019.

[4] Techmer PM. Branch Technology and Foster + Partners win first prize in NASA's 3-D Printed Habitat Challenge using materials designed by Techmer PM. https://www.inda.org/membership/member-news/branch-technology-and-foster-partners-win-first-prize-in-nasas-3-d-printed-habitat-challenge-using-materials-designed-by-techmer-pm/

[5] R. P. Mueller, T. J. Prater, M. Roman, et al. NASA Centennial Challenge: Three Dimensional (3D) Printed Habitat, Phase 3. In *70th International Astronautical Congress (IAC), Washington, D.C.* 2019. 13 p. https://ntrs.nasa.gov/api/citations/20190032475/downloads/20190032475.pdf

[6] B. O'Neal. Dubai inaugurates first 3D printed office building, constructed in 17 days. https://3dprint.com/126426/3d-printed-museum-office/

[7] M. Alawneh, M. Matarneh, S. El-Ashri. The world's first 3D–printed office building in Dubai, 2018. https://www.pci.org/PCI_Docs/Papers/2018/32_Final_Paper.pdf

[8] O. Bari. Build your own 3D printed house, all in one day, 2017. [2020-11-03]. https://www.archdaily.com/806742/build-your-own-3d-printed-house-all-in-one-day

[9] B. Furet, P. Poullain, S. Garnier. 3D printing for construction based on a complex wall of polymer-foam and concrete. *Additive Manufacturing* **28**:58–64, 2019. https://doi.org/10.1016/j.addma.2019.04.002

[10] C. Joh, J. Lee, T. Q. Bui, et al. Buildability and mechanical properties of 3D printed concrete. *Materials* **13**(21):4919, 2020. https://doi.org/10.3390/ma13214919

[11] Master Builders Solutions CZ. MasterFlow 3D 100. https://assets.master-builders-solutions.com/cs-cz/tl_masterflow_3d_100_mbs.pdf

[12] R. J. M. Wolfs, F. P. Bos, T. A. M. Salet. Hardened properties of 3D printed concrete: The influence of process parameters on interlayer adhesion. *Cement and Concrete Research* **119**:132–140, 2019. https://doi.org/10.1016/j.cemconres.2019.02.017

[13] V. N. Nerella, S. Hempel, V. Mechtcherine. Effects of layer-interface properties on mechanical performance of concrete elements produced by extrusion-based 3D-printing. *Construction and Building Materials* **205**:586–601, 2019. https://doi.org/10.1016/j.conbuildmat.2019.01.235